

# The Theory of Complex Angular Momenta

Gribov Lectures on Theoretical Physics

V. N. GRIBOV



PUBLISHED BY THE PRESS SYNDICATE OF THE UNIVERSITY OF CAMBRIDGE  
The Pitt Building, Trumpington Street, Cambridge, United Kingdom

CAMBRIDGE UNIVERSITY PRESS  
The Edinburgh Building, Cambridge CB2 2RU, UK  
40 West 20th Street, New York, NY 10011-4211, USA  
477 Williamstown Road, Port Melbourne, VIC 3207, Australia  
Ruiz de Alarcón 13, 28014 Madrid, Spain  
Dock House, The Waterfront, Cape Town 8001, South Africa

<http://www.cambridge.org>

© V. N. Gribov 2003

This book is in copyright. Subject to statutory exception  
and to the provisions of relevant collective licensing agreements,  
no reproduction of any part may take place without  
the written permission of Cambridge University Press.

First published 2003

Printed in the United Kingdom at the University Press, Cambridge

*A catalogue record for this book is available from the British Library*

ISBN 0 521 81834 6 hardback

# Contents

<i>Foreword by Yuri Dokshitzer</i>	xi
<b>Introduction by Yuri Dokshitzer and Leonid Frankfurt</b>	<b>1</b>
References	6
<b>1 High energy hadron scattering</b>	<b>8</b>
1.1 Basic principles	8
1.1.1 Invariant scattering amplitude and cross section	8
1.1.2 Analyticity and causality	9
1.1.3 Singularities	9
1.1.4 Crossing symmetry	10
1.1.5 The unitarity condition for the scattering matrix	10
1.2 Mandelstam variables for two-particle scattering	10
1.2.1 The Mandelstam plane	11
1.2.2 Threshold singularities on the Mandelstam plane	12
1.3 Partial wave expansion and unitarity	13
1.3.1 Threshold behaviour of partial wave amplitudes	15
1.3.2 Singularities of $\text{Im } A$ on the Mandelstam plane (Karplus curve)	15
1.4 The Froissart theorem	17
1.5 The Pomeranchuk theorem	19
<b>2 Physics of the <math>t</math>-channel and complex angular momenta</b>	<b>22</b>
2.1 Analytical continuation of the $t$ -channel unitarity condition	23
2.1.1 The Mandelstam representation	27
2.1.2 Inconsistency of the ‘black disk’ model of diffraction	28
2.2 Complex angular momenta	29
2.3 Partial wave expansion and Sommerfeld–Watson representation	30
2.4 Continuation of partial wave amplitudes to complex $\ell$	33

2.4.1	Non-relativistic quantum mechanics	33
2.4.2	Relativistic theory	34
2.5	Gribov–Froissart projection	35
2.6	$t$ -Channel partial waves and the black disk model	38
<b>3</b>	<b>Singularities of partial waves and unitarity</b>	<b>39</b>
3.1	Continuation of partial waves with complex $\ell$ to $t < 0$	40
3.1.1	Threshold singularity and partial waves $\phi_\ell$	41
3.1.2	$\phi_\ell(t)$ At $t < 0$ and its discontinuity	42
3.2	The unitarity condition for partial waves with complex $\ell$	43
3.3	Singularities of the partial wave amplitude	44
3.3.1	Left cut in non-relativistic theory	44
3.3.2	Fixed singularities	46
3.3.3	Moving singularities	46
3.4	Moving poles and resonances	48
<b>4</b>	<b>Properties of Regge poles</b>	<b>51</b>
4.1	Resonances	51
4.2	Bound states	53
4.3	Elementary particle or bound state?	53
4.3.1	Regge trajectories	54
4.3.2	Regge pole exchange and particle exchange ( $t > 0$ )	54
4.3.3	Regge exchange and elementary particles ( $t < 0$ )	56
4.3.4	There is no elementary particle with $J > 1$	57
4.3.5	Asymptotics of $s$ -channel amplitudes and reggeization	57
4.4	Factorization	58
<b>5</b>	<b>Regge poles in high energy scattering</b>	<b>61</b>
5.1	$t$ -Channel dominance	61
5.2	Elastic scattering and the pomeron	64
5.2.1	Quantum numbers of the pomeron	64
5.2.2	Slope of the pomeron trajectory	65
5.3	Shrinkage of the diffractive cone	66
5.3.1	$s$ -Channel partial waves in the impact parameter space	66
5.4	Relation between total cross sections	69
<b>6</b>	<b>Scattering of particles with spin</b>	<b>71</b>
6.1	Vector particle exchange	72
6.2	Scattering of nucleons	75
6.2.1	Reggeon quantum numbers and $N\bar{N} \rightarrow$ reggeon vertices	75
6.2.2	Vacuum pole in $\pi N$ and $NN$ scattering	76
6.3	Conspiracy	77

<b>7</b>	<b>Fermion Regge poles</b>	<b>79</b>
7.1	Backward scattering as a relativistic effect	81
7.2	Pion–nucleon scattering	82
7.2.1	Parity in the $u$ -channel	84
7.2.2	Fermion poles with definite parity and singularity at $u = 0$	85
7.2.3	Oscillations in the fermion pole amplitude	87
7.3	Reggeization of a neutron	89
<b>8</b>	<b>Regge poles in perturbation theory</b>	<b>90</b>
8.1	Scattering of a particle in an external field	90
8.2	Scalar field theory $g\phi^3$	90
8.2.1	$g\phi^3$ Theory in the Duffin–Kemmer formalism	91
8.2.2	Analytic properties of the amplitudes	93
8.2.3	Order $g^4 \ln s$	97
8.2.4	Order $g^6 \ln^2 s$	101
8.2.5	Ladder diagrams in all orders	104
8.2.6	Non-ladder diagrams	105
8.3	Interaction with vector mesons	106
<b>9</b>	<b>Reggeization of an electron</b>	<b>112</b>
9.1	Electron exchange in $\mathcal{O}(g^6)$ Compton scattering amplitude	113
9.2	Electron Regge poles	115
9.2.1	Conspiracy in perturbation theory	115
9.2.2	Reggeization in QED (with massless photon)	117
9.3	Electron reggeization: nonsense states	118
<b>10</b>	<b>Vector field theory</b>	<b>121</b>
10.1	Rôle of spin effects in reggeization	122
10.1.1	Nonsense states in the unitarity condition	123
10.1.2	Iteration of the unitarity condition	125
10.1.3	Nonsense states from the $s$ - and $t$ -channel points of view	125
10.1.4	The $j = \frac{1}{2}$ pole in the perturbative nonsense–nonsense amplitude	129
10.2	QED processes with photons in the $t$ -channel	131
10.2.1	The vacuum channel in QED	132
10.2.2	The problem of the photon reggeization	134
<b>11</b>	<b>Inconsistency of the Regge pole picture</b>	<b>137</b>
11.1	The pole $\ell = -1$ and restriction on the amplitude fall-off	137
11.2	Contradiction with unitarity	141
11.3	Poles condensing at $\ell = -1$	142
11.3.1	Amplitude cannot fall faster than $1/s$	143

11.4	Particles with spin: failure of the Regge pole picture	143
<b>12</b>	<b>Two-reggeon exchange and branch point singularities in the <math>\ell</math> plane</b>	<b>145</b>
12.1	Normalization of partial waves and the unitarity condition	145
12.1.1	Redefinition of partial wave amplitudes	145
12.1.2	Particles with spin in the unitarity condition	146
12.2	Particle scattering via a two-particle intermediate state	148
12.3	Two-reggeon exchange and production vertices	150
12.4	Asymptotics of two-reggeon exchange amplitude	153
12.5	Two-reggeon branching and $\ell = -1$	154
12.6	Movement of the branching in the $t$ and $j$ planes	156
12.7	Signature of the two-reggeon branching	157
<b>13</b>	<b>Properties of Mandelstam branch singularities</b>	<b>159</b>
13.1	Branchings as a generalization of the $\ell = -1$ singularity	159
13.1.1	Branchings in the $j$ plane	159
13.1.2	Branch singularity in the unitarity condition	160
13.2	Branchings in the vacuum channel	161
13.2.1	The pattern of branch points in the $j$ plane	162
13.2.2	The Mandelstam representation in the presence of branchings	162
13.3	Vacuum–non-vacuum pole branchings	163
13.4	Experimental verification of branching singularities	165
13.4.1	Branchings and conspiracy	166
<b>14</b>	<b>Reggeon diagrams</b>	<b>168</b>
14.1	Two-particle–two-reggeon transition amplitude	172
14.1.1	Structure of the vertex	172
14.1.2	Analytic properties of the vertex	173
14.1.3	Factorization	174
14.2	Partial wave amplitude of the Mandelstam branching	175
<b>15</b>	<b>Interacting reggeons</b>	<b>183</b>
<b>16</b>	<b>Reggeon field theory</b>	<b>193</b>
16.1	Enhanced reggeon diagrams	195
16.2	Effective field theory of interacting reggeons	200
16.3	Equation for the Green function $G$	201
16.4	Equation for the vertex function $\Gamma_2$	202
16.5	Weak and strong coupling regimes	204
16.6	Pomeron Green function and reggeon unitarity condition	205

<b>17</b>	<b>The structure of weak and strong coupling solutions</b>	<b>208</b>
17.1	Weak coupling regime	208
17.1.1	The Green function	208
17.1.2	$P \rightarrow PP$ vertex	209
17.1.3	Induced multi-reggeon vertices	211
17.1.4	Vanishing of multi-reggeon couplings	213
17.2	Problems of the strong coupling regime	215
<b>Appendix A: Space-time description of the hadron interactions at high energies</b>		<b>216</b>
A.1	Wave function of the hadron. Orthogonality and normalization	221
A.2	Distribution of the partons in space and momentum	223
A.3	Deep inelastic scattering	227
A.4	Strong interactions of hadrons	231
A.5	Elastic and quasi-elastic processes	235
	References	238
<b>Appendix B: Character of inclusive spectra and fluctuations produced in inelastic processes by multi-pomeron exchange</b>		<b>240</b>
B.1	The absorptive parts of reggeon diagrams in the $s$ -channel. Classification of inelastic processes	244
B.2	Relations among the absorptive parts of reggeon diagrams	247
B.3	Inclusive cross sections	252
B.4	Main corrections to the inclusive cross sections in the central region	255
B.5	Fluctuations in the distribution of the density of produced particles	259
	References	266
<b>Appendix C: Theory of the heavy pomeron</b>		<b>267</b>
C.1	Introduction	267
C.2	Non-enhanced cuts at $\alpha' = 0$	269
C.3	Estimation of enhanced cuts at $\alpha' = 0$	271
C.4	Structure of the transition amplitude of one pomeron - to two	273
C.5	The Green function and the vertex part at $\alpha' = 0$	275
C.6	Properties of high energy processes in the theory with $\alpha' = 0$	282
C.6.1	Two-particle processes, total cross sections	283
C.6.2	Inclusive spectra, multiplicity	284
C.6.3	Correlation, multiplicity distribution	284

	C.6.4 Probability of fluctuations in individual events: the inclusive spectrum in the three-pomeron limit	286
	C.6.5 Multi-reggeon processes	291
C.7	The case $\alpha' \neq 0$	291
C.8	The contribution of cuts at small $\alpha'$	292
C.9	Conclusion	294
	References	295
	Index	296



# 1

## High energy hadron scattering

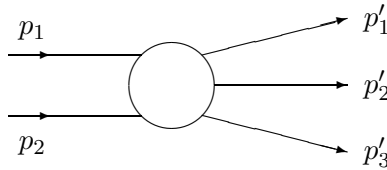
In these lectures the theory of complex angular momenta is presented. It is assumed that readers are familiar with the methods of modern quantum field theory (QFT). Nevertheless we shall briefly recall its basic principles.

### 1.1 Basic principles

The main experimental fact underlying the theory is the existence of strong interactions between particles of non-zero masses. The theory is constructed for quantities which have a direct physical meaning.

#### *1.1.1 Invariant scattering amplitude and cross section*

Such quantities are the scattering amplitudes,



which are supposed to be functions of the kinematical invariants only:  $A(p_1, \dots, p_n) = A(p_i^2, p_i p_k)$ . For simplicity, let us begin by considering the scattering of neutral, spinless particles as shown in Fig. 1.1. We use a normalization of the scattering amplitudes such that the kinematical factors arising from the wave functions of the external particles are factorized out. The cross section of any process can be defined in terms of

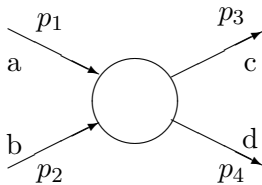


Fig. 1.1. Two-particle scattering

the invariant amplitude  $A$  as follows:

$$d\sigma_n = (2\pi)^4 \delta\left(p_1 + p_2 - \sum_i p'_i\right) |A|^2 \prod_{i=1}^n \frac{d^3 p'_i}{2p'_{i0} (2\pi)^3} \frac{1}{I},$$

$$I = 4p_{10}p_{20}J = 4\sqrt{(p_1 p_2)^2 - m_1^2 m_2^2}. \quad (1.1)$$

Here the factor  $(2\pi)^4 \delta()$  originates from energy-momentum conservation,  $d^3 p'_i / 2p'_{i0} (2\pi)^3$  from the phase space volume;  $I$  is the Møller factor which combines the flux density  $J$  of the initial particles and  $(2p_{10} 2p_{20})^{-1}$  coming from their wave functions.

### 1.1.2 Analyticity and causality

It is assumed that the scattering amplitude  $A$  is an analytic function of its arguments (for instance it cannot contain terms like  $\Theta(p_{i0})$ ). This assumption is a manifestation of the causality principle. Without analyticity, the scattered waves could appear at their source before being emitted. Additionally, it is natural to conjecture at this point that the growth of the scattering amplitude, as one of the invariants tends to infinity for fixed values of the remaining invariants, is polynomially bounded,

$$|A(p_1, \dots, p_n)| < (p_i p_j)^N.$$

This assumption is closely related to causality and the locality of the interaction. One needs it in order to write the dispersion representation for the amplitudes (to be able to close the integration contour over an infinitely large circle).

### 1.1.3 Singularities

It is also assumed that all singularities of the amplitude on the physical sheet have the meaning of reaction thresholds, i.e. they are determined by

physical masses of the intermediate state particles. In terms of Feynman diagrams they are the Landau singularities.

#### 1.1.4 Crossing symmetry

We will clarify the meaning of crossing, taking as an example a four-particle amplitude. Since this amplitude depends on the kinematical invariants (and not on the sign of  $p_{i0}$ ), the same analytic function describes the reaction

$$a(p_1) + b(p_2) \rightarrow c(p_3) + d(p_4) \quad \text{for } p_{10}, p_{20}, p_{30}, p_{40} > 0$$

as well as

$$a(p_1) + \bar{c}(-p_3) \rightarrow \bar{b}(-p_2) + d(p_4) \quad \text{for } p_{10}, p_{40} > 0, p_{20}, p_{30} < 0$$

and

$$a(p_1) + \bar{d}(-p_4) \rightarrow \bar{b}(-p_2) + c(p_3) \quad \text{for } p_{10}, p_{30} > 0, p_{20}, p_{40} < 0.$$

For an unstable particle, there is the additional reaction  $a \rightarrow \bar{b} + c + d$  ( $p_{10}, p_{30}, p_{40} > 0, p_{20} < 0$ ).

In fact, the crossing symmetry implies the *CPT*-theorem – invariance of the amplitude  $A$  with respect to the combination of charge conjugation  $C$ , space reflection  $P$  and time reversal  $T$ .

Crossing symmetry follows from the first three assumptions. It can be shown that the same assumptions allow us to prove the spin-statistics relation theorem (the Pauli theorem).

#### 1.1.5 The unitarity condition for the scattering matrix

Unitarity has a simple physical meaning: the sum of probabilities of all processes which are possible at a given energy is equal to unity,  $SS^+ = 1$ . If  $S = 1 + iA$ , then

$$i(A - A^+) = -AA^+.$$

Representing the amplitude  $A$  as the sum of its real and imaginary parts,  $A = \text{Re } A + i \text{Im } A$ , the unitarity condition takes the form

$$2 \text{Im } A = AA^+. \quad (1.2)$$

### 1.2 Mandelstam variables for two-particle scattering

Let us show how all the above principles work in the case of the four-particle amplitude.

Although the amplitude of the  $2 \rightarrow 2$  process depends evidently on two independent variables, that is the energy of the incoming particles and the scattering angle, it is more convenient to consider  $A$  as a function of three Mandelstam variables

$$s = (p_1 + p_2)^2, \quad t = (p_1 - p_3)^2, \quad u = (p_1 - p_4)^2.$$

They are related to each other by

$$s + t + u = \sum_{i=1}^4 m_i^2$$

where the sum runs over the masses of all particles participating in the collision.

For the sake of simplicity, in what follows we restrict ourselves to the case of equal particle masses,  $m_i = \mu$ .

The Mandelstam variables have a simple physical meaning. For instance, in the centre-of-mass system (cms) of the reaction  $a + b \rightarrow c + d$  (the so-called  $s$ -channel),  $s$  is the square of the total energy of the colliding particles and  $t = -(\mathbf{p}_1 - \mathbf{p}_3)^2$  is the square of the momentum transfer from  $a$  to  $c$ . In the cms of the reaction  $a + \bar{c} \rightarrow \bar{b} + d$  ( $t$ -channel),  $t$  plays the role of the total energy squared, and  $s$  is the square of momentum transfer. The variables  $u$  and  $t$ , respectively, play similar rôles in the  $u$ -channel reaction  $a + \bar{d} \rightarrow \bar{b} + c$ .

### 1.2.1 The Mandelstam plane

It is convenient, following Landau, to represent the kinematics of the three reactions graphically on the Mandelstam plane. We use here the well known geometrical fact that the sum of the distances from a point on the plane to the sides of an equilateral triangle does not depend on the position of the point. Therefore, taking into account the condition  $s + t + u = 4\mu^2$ , let us measure  $s$ ,  $t$  and  $u$  as the distances to the sides of the triangle.

It is easy then to represent the physical region of any reaction on such a plane. For instance, the physical region of the reaction  $a + \bar{c} \rightarrow \bar{b} + d$  corresponds to  $t \geq 4\mu^2$ ,  $s \leq 0$ ,  $u \leq 0$  and it is shown on Fig. 1.2 as the upper shaded area. The physical regions of the other reactions can be identified in a similar manner.

In the case of the scattering of *identical* neutral particles the amplitude in each physical region is the same and it satisfies the unitarity condition separately in each region.

Examining the Mandelstam plane Fig. 1.2 we notice an interesting feature: as we move from positive to negative values of  $s$  (from the physical

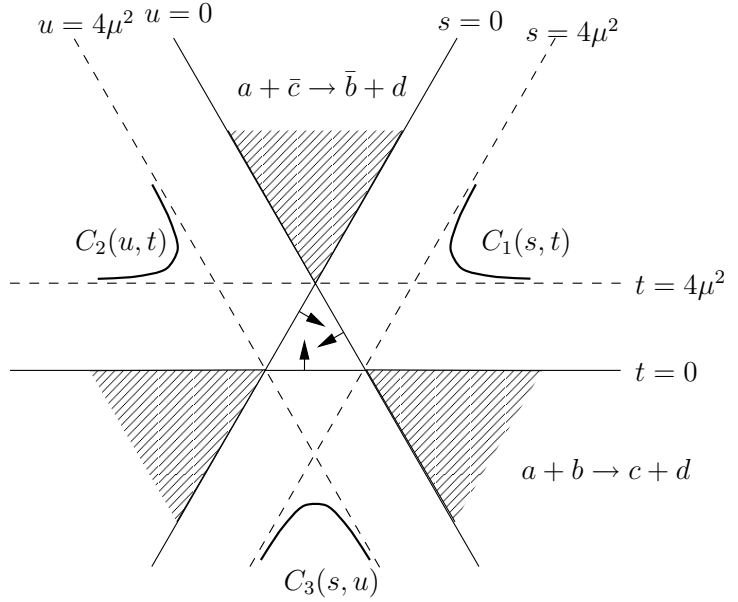


Fig. 1.2. Crossing reactions on the Mandelstam plane

region of the  $s$ -channel to the  $u$ -channel), the energy dependence of the scattering amplitude turns into the angular dependence.

### 1.2.2 Threshold singularities on the Mandelstam plane

Let us discuss now singularities of the amplitude. As an illustration, we consider elastic scattering of neutral pions:  $\pi^0 + \pi^0 \rightarrow \pi^0 + \pi^0$ . We will assume that (in accordance with experiment) pions are the lightest stable hadrons and that there is no bound state of two neutral pions. Then, the amplitude has no singularities at  $s < 4\mu^2$ . The first threshold lies at  $s = (2\mu)^2$ . It corresponds to the two-particle intermediate state. The next, three-particle threshold could have appeared at  $s = (3\mu)^2$ . In reality, the second threshold in the pion scattering amplitude is situated at  $s = (4\mu)^2$  – the four-particle state, since the transition of two pions into three is forbidden by  $G$ -parity conservation.

Similar singularities in *energy* are known to appear in quantum mechanics, for instance the threshold singularity at  $s \rightarrow 4\mu^2$ .

There is however a principal difference between relativistic and non-relativistic theories in the interpretation of the singularities in *momentum transfer*.

In quantum mechanics such singularities are determined by the poten-

tial. For instance, the Yukawa potential

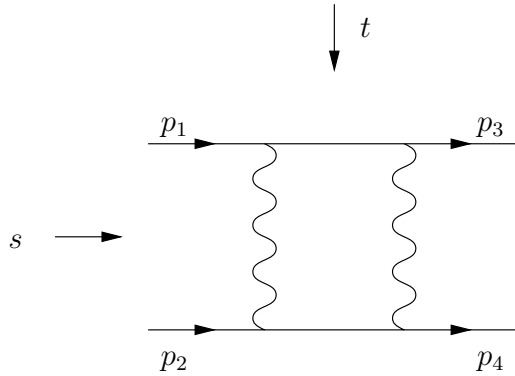
$$V(r) \propto \frac{\exp(-\alpha r)}{r}$$

corresponds to a pole of the scattering amplitude in the plane of the squared momentum transfer  $k$ :

$$A(k^2) \propto \frac{1}{k^2 + \alpha^2}.$$

In the relativistic theory the rôle of the potential is played by energy singularities in the  $t$ -channel, thresholds at  $t = 4\mu^2$ ,  $16\mu^2$  and so on.

Let us illustrate this statement by considering the box diagram



whose contribution we may interpret as defining the potential in the *next-to-Born* approximation. It is easy to see that the radius of this potential is  $r = 1/2\mu$ .

Thus, the assumption that all the singularities of the scattering amplitude are determined by the masses of real particles implies that there are no potentials with an infinite radius (since all hadrons have non-zero masses).

### 1.3 Partial wave expansion and unitarity

In order to obtain more concrete results, we must exploit analyticity and unitarity of the  $S$ -matrix.

Due to conservation of angular momentum, the unitarity condition for scattering amplitudes with given angular momentum  $\ell$  becomes diagonal. It is convenient, therefore, to expand the  $s$ -channel amplitude into partial waves:

$$A(s, t) = \sum_{\ell=0}^{\infty} f_{\ell}(s)(2\ell + 1)P_{\ell}(z), \quad (1.3a)$$

where  $P_\ell(z)$  is the Legendre polynomial and  $z$  is the cosine of the scattering angle:

$$z = \cos \Theta_s = 1 + \frac{2t}{s - 4\mu^2} = \frac{u - t}{u + t}. \quad (1.3b)$$

From (1.3b) it becomes obvious that in the physical region of  $s$ -channel ( $t, u \leq 0$ ) we have  $-1 \leq z \leq 1$ , as expected.

Substituting the expansion (1.3a) into (1.2) and using well known orthogonality properties of Legendre polynomials, it is straightforward to derive the unitarity condition for partial amplitudes  $f_\ell(s)$ . It acquires a particularly simple form\*

$$\text{Im } f_\ell(s) = \frac{k_s}{16\pi\omega_s} f_\ell(s) f_\ell^*(s) + \Delta, \quad (1.4a)$$

where  $p$  and  $\omega$  stand for cms particle momentum and energy, respectively,

$$k_s = \frac{\sqrt{s - 4\mu^2}}{2}, \quad \omega_s = \frac{\sqrt{s}}{2}. \quad (1.4b)$$

In (1.4a)  $\Delta$  represents the contribution of the inelastic channels,  $\Delta > 0$ . The elastic case,  $\Delta = 0$ , can be solved explicitly:

$$f_\ell(s) = i \frac{8\pi}{v} \left[ 1 - e^{2i\delta_\ell(s)} \right], \quad v = \frac{k_s}{\omega_s}, \quad (1.5a)$$

with  $\delta_\ell$  the scattering phase.

The solution of the elastic unitarity condition has the same form as in non-relativistic quantum mechanics except for the velocity factor  $v = k/\omega$  which arises due to relativistic normalization of the amplitude  $A$ .

In the general case the solution of (1.4a) can be parametrized with the help of the ‘elasticity parameter’  $\eta_\ell(s) \leq 1$ :

$$f_\ell(s) = i \frac{8\pi}{v} \left[ 1 - \eta_\ell \cdot e^{2i\delta_\ell} \right], \quad \eta_\ell^2 = 1 - \frac{v}{4\pi} \Delta. \quad (1.5b)$$

From (1.5) it follows that partial wave amplitudes are bounded from above:

$$\text{Im } f_\ell \leq |f_\ell| \leq 16\pi v^{-1} \quad (\eta_\ell = 1). \quad (1.6a)$$

Maximal inelasticity of the scattering in a given partial wave corresponds to  $\eta_\ell = 0$ . In the high energy limit this leads to the restriction

$$\text{Im } f_\ell \leq |f_\ell| \leq 8\pi \quad (\eta_\ell = 0). \quad (1.6b)$$

---

\* Actual derivation of the unitarity condition for partial wave amplitudes uses the relation between the angles of initial, intermediate and final state particles and the known orthogonality properties of Legendre polynomials.

In this case the amplitude (1.5b) is purely imaginary, so that the elastic scattering is but a ‘shadow’ of inelastic channels. The model

$$f_\ell = \begin{cases} i \frac{8\pi}{v}, & \eta_\ell = 0, & \text{for } \ell < \ell_0 = k_s R, \\ 0, & \eta_\ell = 1, \delta_\ell = 0, & \text{for } \ell > \ell_0, \end{cases}$$

is known as the ‘black disk’ model for diffractive scattering. At high energies  $s \simeq 4k_s^2 \gg \mu^2$  ( $v \simeq 1$ ) when  $\ell_0 \gg 1$ , it leads to the forward scattering amplitude (see (1.3a))

$$A(s, 0) = \sum_{\ell} (2\ell + 1) f_\ell \simeq \ell_0^2 \cdot 8\pi i \simeq i s \cdot 2\pi R^2,$$

which, according to the optical theorem, results in

$$\sigma_{\text{tot}} = \frac{\text{Im } A(s, 0)}{v s} \simeq 2\pi R^2 = \pi R^2|_{\text{inelastic}} + \pi R^2|_{\text{diffraction}}.$$

This is the pattern of diffraction off an absorbing disk of radius  $R$ .

### 1.3.1 Threshold behaviour of partial wave amplitudes

It is well known from quantum mechanics that for potentials of finite range,  $r_0$ , the partial waves behave like  $(kr_0)^\ell$  as  $k \rightarrow 0$ . It can be easily seen that a similar result holds in the theory of the  $S$  matrix.

Indeed, the singularity in  $t$  of the amplitude  $A(s, t)$ , the closest to the physical region in the  $s$ -channel, is located at  $t = 4\mu^2$ . Therefore the series (1.3a) should be convergent for  $z$  up to  $z_0 = 1 + 4\mu^2/2k_s^2$ .

For  $t > 0$  and  $s \rightarrow 4\mu^2$ , one gets  $z \rightarrow \infty$  and  $P_\ell(z)$  grows as  $P_\ell(z) \sim z^\ell$ . For the series (1.3a) to converge, one has to require that  $f_\ell$  should fall with  $\ell$  like  $(2k_s^2/4\mu^2)^\ell$  but not faster since at  $t = 4\mu^2$  the series has to be divergent.

### 1.3.2 Singularities of $\text{Im } A$ on the Mandelstam plane (Karplus curve)

Repeating the same arguments for the *imaginary part* of the  $s$ -channel amplitude  $\text{Im } A$  we would get

$$\text{Im } f_\ell(s) \propto k_s^{2\ell}, \quad k_s \rightarrow 0.$$

This cannot be true, however, since it contradicts the unitarity condition:  $\text{Im } f_\ell \propto k_s^{4\ell+1}$  follows from (1.4a). Substituting this behaviour into (1.3a), we observe that the series for  $\text{Im}_s A(s, t)$  remains convergent at  $t = \mu^2$ . We conclude that singularities in  $t$  of the *imaginary part* of the amplitude are located *above*  $t = 4\mu^2$ , and their position depends on  $s$ .



Actually, using the unitarity condition one can find the exact form of the line of singularities of  $\text{Im}_s A(s, t)$  on the Mandelstam plane, known as Karplus (or Landau) curve.

Let us sketch its derivation in the region  $4\mu^2 \leq s \leq 16\mu^2$ ,  $t > 4\mu^2$  where the two-particle unitarity condition is valid ( $\Delta = 0$  in (1.4a)).

For  $t > 0$  we have  $z > 1$  and the Legendre polynomials increase exponentially with  $\ell$ :

$$P_\ell(\cosh \alpha) \stackrel{\ell \rightarrow \infty}{\simeq} \frac{e^{(\ell + \frac{1}{2})\alpha}}{\sqrt{2\pi\ell \sinh \alpha}}, \quad \cosh \alpha \equiv z = 1 + \frac{t}{2k_s^2} > 1. \quad (1.7)$$

To ensure convergence of (1.3a) for  $t < 4\mu^2$ , partial waves have to fall as

$$f_\ell \sim e^{-\ell\alpha_0}, \quad \cosh \alpha_0 = 1 + \frac{4\mu^2}{2k_s^2}. \quad (1.8)$$

Due to the unitarity condition (1.4a) the imaginary part falls even faster:  $\text{Im } f_\ell \sim \exp(-2\ell\alpha_0)$ .

Consider now the series (1.3a) for  $\text{Im}_s A(s, t)$ . With  $t$  increasing, the growing factor  $\exp(\ell\alpha)$ , originating from the Legendre polynomials, eventually overtakes the falling factor  $\exp(-2\ell\alpha_0)$  due to  $\text{Im } f_\ell$ . At this point the series becomes divergent, and  $\text{Im}_s A(s, t)$  develops a singularity.

Thus, the line of singularities of  $\text{Im}_s A(s, t)$  for  $4\mu^2 \leq s \leq 16\mu^2$  is given by the equation  $\alpha = 2\alpha_0$ . In terms of the variables  $s$  and  $t$  this equation takes the form

$$\frac{t}{16\mu^2} = \frac{s}{s - 4\mu^2}, \quad 4\mu^2 \leq s \leq 16\mu^2.$$

In the complementary region  $4\mu^2 \leq t \leq 16\mu^2$ ,  $s \geq 4\mu^2$ , the Karplus curve can be found using the symmetry of  $A(s, t)$  under the permutation  $s \leftrightarrow t$ :

$$\frac{s}{16\mu^2} = \frac{t}{t - 4\mu^2}, \quad 4\mu^2 \leq t \leq 16\mu^2.$$

This example illustrates how the unitarity condition determines the analyticity domain of the scattering amplitude.

The lines of singularities  $C_i$  of the amplitude  $A(s, t)$  are drawn on the Mandelstam plane in Fig. 1.2.

The fact that the Karplus curve  $C_1(s, t)$  has finite asymptotes (in our example, the lines  $s = 4\mu^2$ ,  $t \rightarrow \infty$ , and  $t = 4\mu^2$ ,  $s \rightarrow \infty$ ) is obvious, since otherwise the partial wave amplitudes would decrease with increasing  $\ell$  faster than any exponential, which is in contradiction with the standard behaviour  $f_\ell \sim \exp(-\alpha\ell)$  for  $\ell \rightarrow \infty$ .

In reality, the Karplus curves for  $\pi\pi$  scattering are not symmetric with respect to  $s$  and  $t$ , which is a consequence of the pions being pseudoscalars (see the following lectures and the footnote on page 27).

### 1.4 The Froissart theorem

In 1958 Froissart showed that the analytic properties of the scattering amplitude together with the unitarity condition put certain restrictions on the asymptotic behaviour of  $A(s, t)$  in the physical region. Let us show that asymptotically

$$\operatorname{Im} A(s, t)|_{t=0} \leq \text{const} \cdot s \ln^2 \frac{s}{s_0}, \quad s \rightarrow \infty.$$

First let us estimate  $f_\ell$  at large  $s$  using the fact that the singularity of  $\operatorname{Im}_s A(s, t)$  closest to the physical region of the  $s$ -channel is situated at  $t = 4\mu^2$ . As was shown above, at large  $\ell$  the partial wave amplitude falls exponentially. Since for  $k_s^2 \propto s \gg t$  (1.8) gives  $\alpha \simeq \sqrt{t}/k_s$ , we have

$$f_\ell(s) \simeq c(s, \ell) \exp\left(-\frac{\ell}{k_s} \sqrt{4\mu^2}\right), \quad \ell, s \rightarrow \infty, \quad (1.9)$$

where  $c(s, \ell)$  is slowly (non-exponentially) varying with  $\ell$ .

Let us now assume that for  $t$  arbitrarily close to  $4\mu^2$  the amplitude grows with  $s$  not faster than some power. Then the same is valid for  $\operatorname{Im} c(s, \ell)$ . Indeed,  $\operatorname{Im} f_\ell$  is positive due to the unitarity condition, and so is  $P_\ell(1 + t/2k_s^2)$  for  $t \geq 0$ . Therefore for each partial wave we have an estimate<sup>†</sup>

$$\begin{aligned} \left(\frac{s}{s_0}\right)^N &> \operatorname{Im} A(s, t) = \sum_{\ell=0}^{\infty} \operatorname{Im} f_\ell(s) (2\ell + 1) P_\ell\left(1 + \frac{t}{2k_s^2}\right) \\ &> \operatorname{Im} c(s, \ell) \left(2\pi\ell \frac{\sqrt{t}}{k_s}\right)^{-1/2} \exp\left\{\frac{\ell}{k_s} \left(\sqrt{t} - \sqrt{4\mu^2}\right)\right\}. \end{aligned} \quad (1.10)$$

Since (1.10) holds for arbitrary positive  $t < 4\mu^2$ , we conclude that

$$\operatorname{Im} c(s, \ell) < (s/s_0)^N,$$

and finally, modulo an irrelevant pre-exponential factor,

$$\operatorname{Im} f_\ell(s) \lesssim \left(\frac{s}{s_0}\right)^N \exp\left(-\frac{2\mu}{k_s} \ell\right). \quad (1.11)$$

(Using the unitarity condition one can derive a similar estimate for  $\operatorname{Re} f_\ell$ .)

---

<sup>†</sup> the series converges inside the so-called Lehman ellipse in the  $z$  plane

We are now in a position to estimate the imaginary part of the forward scattering amplitude:

$$\begin{aligned} \operatorname{Im} A(s, t=0) &= \sum_{\ell=0}^{\infty} \operatorname{Im} f_{\ell}(s) (2\ell+1) \\ &\leq 8\pi \sum_{\ell=0}^L (2\ell+1) + \sum_{\ell=L+1}^{\infty} \operatorname{Im} f_{\ell}(s) (2\ell+1). \end{aligned} \quad (1.12)$$

Here we have extracted the finite sum  $\ell < L$  in which partial waves are large,  $\operatorname{Im} f_{\ell} \simeq |f_{\ell}| = \mathcal{O}(1)$ , and estimated its contribution from above by substituting for  $\operatorname{Im} f_{\ell}$  its maximal value allowed by unitarity, see (1.6b):

$$\sum_{\ell=0}^L (2\ell+1) \simeq L^2.$$

The border value of the angular momentum  $L$  above which partial wave amplitudes become small,  $\operatorname{Im} f_{\ell > L} \ll 1$ , and fall exponentially with  $\ell$  according to (1.11) can be found by setting

$$\left(\frac{s}{s_0}\right)^N \exp\left(-\frac{2\mu}{k_s} L\right) \simeq 1 \quad \Rightarrow \quad L \simeq \frac{k_s}{2\mu} \ln \frac{s}{s_0}.$$

The contribution of the infinite tail of the series in (1.12) can be estimated using  $f_{L+n} \sim f_L \exp(-2\mu n/k_s)$  and turns out to be subdominant:

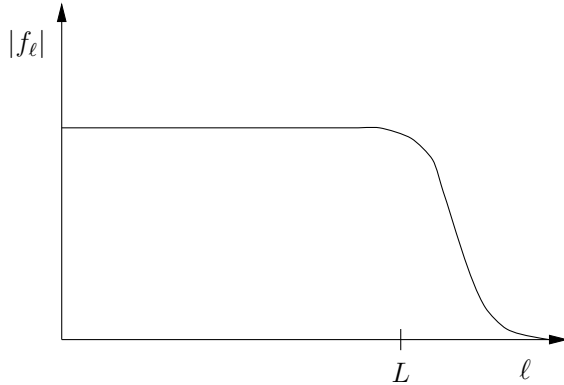
$$\sum_{n=0}^{\infty} 2(L+n) \exp\left\{-\frac{2\mu}{k_s} n\right\} \simeq \frac{k_s}{\mu} L + \frac{k_s^2}{2\mu^2} \stackrel{s \rightarrow \infty}{\ll} L^2.$$

Thus,

$$\operatorname{Im} A(s, t=0) \propto L^2 \propto s \ln^2 \frac{s}{s_0}.$$

This is the Froissart theorem.

The magnitude of the partial wave as a function of  $\ell$  is sketched here:



Since according to the optical theorem  $\text{Im } A(s, t = 0) = s\sigma_{\text{tot}}(s)$ , it follows from the Froissart theorem that the total cross section cannot grow with the centre of mass energy  $\sqrt{s}$  faster than the squared logarithm of  $s$ ,  $\sigma_{\text{tot}}(s) \leq \sigma_0 \ln^2(s/s_0)$ , and the interaction radius cannot grow faster than the logarithm of  $s$ .

An analogous consideration, together with the unitarity condition, leads to the similar inequality for the *real* part of the forward scattering amplitude,  $|\text{Re } A(s, t = 0)| < \text{const} \cdot s \ln^2(s/s_0)$ .

In order for the cross section not to decrease with increasing energy, the amplitude  $A(s, t = 0)$  has to grow and, as a consequence, the number of partial waves contributing to the sum in (1.3a) has to be large. This allows us to replace the sum in (1.3a) by the integral over  $\ell$ , using the well known approximate expression for the Legendre polynomials,

$$P_\ell(\cos \Theta) \simeq J_0 \left[ (2\ell + 1) \frac{\Theta}{2} \right], \quad \ell \gg 1, \quad \theta \ll 1. \quad (1.13)$$

We obtain

$$A(s, t) \simeq \int f_\ell(s) J_0 \left[ (2\ell + 1) \frac{\Theta}{2} \right] (2\ell + 1) d\ell.$$

It is convenient to replace  $\ell$  by the impact parameter  $\rho$ ,  $\ell + 1/2 = k_s \rho$ . Then, using  $t \simeq -(k_s \Theta)^2$ , we obtain

$$A(s, t) \simeq k_s^2 \int f(\rho, s) J_0(\rho \sqrt{-t}) 2\rho d\rho. \quad (1.14)$$

If the values of  $\rho$  giving the dominant contribution to this integral do not depend on  $s$  (which is the case for the usual picture of diffractive scattering off a finite size object), then it is natural to expect that the amplitude takes the factorized form  $A(s, t) \simeq a(s)F(t)$ . If we additionally assume that the partial wave amplitudes  $f(\rho, s)$  that are dominant in (1.11) approach constant values as  $s \rightarrow \infty$ , then  $A(s, t) \sim sF(t)$  and the total cross section tends to a constant.

## 1.5 The Pomeranchuk theorem

In 1958 I.Ya. Pomeranchuk showed that if the total cross sections are constant at high energies, then the total cross sections of the scattering of a particle and its antiparticle off the same target should be asymptotically equal. The derivation of this result is based on the properties of the scattering amplitude in the  $s$ - and  $u$ -channels.

Let us identify the singularities of  $A(s, t = 0)$  in the complex  $s$  plane. They are the right-hand cut  $s \geq 4\mu^2$  and the left-hand cut  $s \leq 0$ . The latter cut corresponds to the right-hand cut  $u \geq 4\mu^2$  in the complex  $u$  plane due to the relation  $s + t + u = 4\mu^2$ .

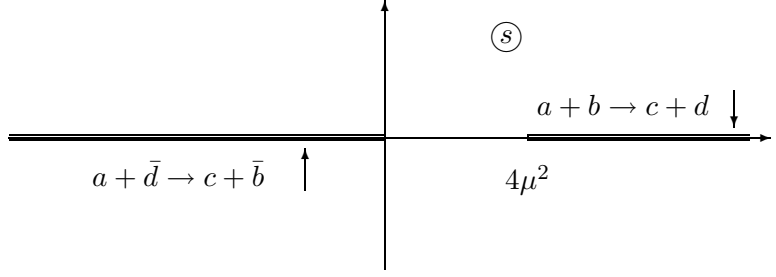


Fig. 1.3. Amplitudes of two crossing reactions in the complex  $s$  plane

It is natural to assume that the amplitude of the reaction  $a + b \rightarrow c + d$  is equal to the value  $A(s, t)$  on the upper edge of the right cut in  $s$ , which corresponds to the usual definition of Feynman integrals in perturbation theory:

$$A(a + b \rightarrow c + d) \rightarrow \lim_{\varepsilon \rightarrow 0} A(s + i\varepsilon, t).$$

Similarly, the physical amplitude of the reaction  $a + \bar{d} \rightarrow c + \bar{b}$  is given by the value of  $A$  on the upper edge of the right-hand cut in  $u$ , i.e.

$$A(a + \bar{d} \rightarrow c + \bar{b}) = \lim_{\varepsilon \rightarrow 0} A(u + i\varepsilon, t) = \lim_{\varepsilon \rightarrow 0} A(-(s - i\varepsilon) - t + 4\mu^2, t),$$

where the latter equality follows from the identity  $s + t + u = 4\mu^2$  together with crossing symmetry. Thus the physical amplitude of the cross-channel reaction in the  $s$  plane is obtained by approaching the cut  $s \leq 0$  from below, as shown in Fig. 1.3. Furthermore, since  $A(s, t \leq 0)$  is real on the interval  $0 < s < 4\mu^2$  which is free from singularities, the values of the amplitude on the two edges of the cut are complex conjugate. Therefore we may use the relation  $A(s - i\varepsilon, t < 0) = A^*(s + i\varepsilon, t < 0)$  to finally arrive at

$$A_{a+\bar{d} \rightarrow c+\bar{b}}(s) \simeq [A_{a+b \rightarrow c+d}(-s)]^*, \quad s \simeq -u. \quad (1.15)$$

Pomeranchuk proved the theorem under the assumption that the elastic scattering amplitude at large  $s$  has the form

$$A_{a+b \rightarrow a+b} = s F(t), \quad (1.16a)$$

so that the total cross section tends to a constant at  $s \rightarrow \infty$ . Using the relation (1.15) we then obtain

$$A_{a+\bar{b} \rightarrow a+\bar{b}} = -s F^*(t), \quad (1.16b)$$

yielding that the imaginary parts of the two amplitudes are equal whereas their real parts have opposite signs. (This implies that in such a model the part of the amplitude that is symmetric in  $s, u$  must be purely imaginary

while the antisymmetric part must be real.) Since the total cross section is defined by the imaginary part of  $A$ , the Pomeranchuk theorem follows suit:

$$\sigma_{\text{tot}}(a+b) = \sigma_{\text{tot}}(a+\bar{b}).$$

If the total cross sections *increase* with energy, the asymptotic equality of  $\sigma_{ab}$  and  $\sigma_{a\bar{b}}$  cannot, in general, be proved. The Pomeranchuk theorem, however, can be proved, assuming asymptotic factorization of the amplitude,  $A(s, t) \simeq a(s)F(t)$ , for a special class of the energy behaviour, namely,  $a(s) = s(\ln s)^\beta$ . To carry out the proof one must use the hypothesis that asymptotically the real part of the amplitude does not exceed its imaginary part

$$\lim_{s \rightarrow \infty} \frac{\text{Re } A(s, t)}{\text{Im } A(s, t)} < \text{const.} \quad (1.17)$$

It is supported by the observation that in general  $\text{Re } f_\ell$  is a sign alternating function so that destructive interference in the series (1.3a) for  $\text{Re } A(s, t)$  is possible. (Here it is important, once again, that at high energies the large values of  $\ell$  are essential.)

We may illustrate the nature and significance of this hypothesis on a simple example. Consider an amplitude of the form

$$A(s, t) = s \ln \frac{-s}{s_0} \cdot c(t)$$

with  $c(t)$  a real function. For  $s > 0$  this amplitude is complex, and the cross section in the  $s$ -channel is constant, whereas at negative  $s$  (positive  $u$ ) we have  $\text{Im } A = 0$  and the  $u$ -channel cross section vanishes.

Did we manage to construct a counterexample to the Pomeranchuk theorem? Obviously not, since our model amplitude is not realistic. It gives rise to the elastic cross section exceeding the total cross section,

$$\sigma_{\text{el}} \sim \int \frac{dt}{s^2} |A(s, t)|^2 \propto \ln^2 s \gg \sigma_{\text{tot}} \sim \text{const},$$

which is a consequence of  $\text{Re } A/\text{Im } A \sim \ln s \rightarrow \infty$ , in contradiction with (1.17).

In this lecture we have demonstrated simple consequences of the analyticity and crossing symmetry of the scattering amplitude.

In the forthcoming lectures we will show how the  $t$ -channel unitarity can be used to study the asymptotics of the scattering amplitudes for  $s \rightarrow \infty$ . It is singularities of the amplitude in  $t$  (rather than those in  $u$ ) that are located close to the physical region in the  $s$ -channel on the Mandelstam plane. This explains why the physics of the  $t$ -channel is important for large  $s$ .